Finite Element Analysis of Dispersion in Waveguides with Sharp Metal Edges

J. P. WEBB, MEMBER, IEEE

Abstract—**The dispersion characteristics of arbitrarily shaped waveguides with sharp metal edges are found by a finite element method in which the usual polynomials are supplemented by singular trial functions. As in recent approaches, the method solves for the three components of the magnetic field and can thereby avoid spurious modes. Results are presented for a rectangular waveguide with two double ridges and for shielded microstrip on isotropic and anisotropic substrates.**

I. Introduction

WAVEGUIDES with sharp metal edges are widely used at microwave frequencies; examples are ridge guide, microstrip, slotline and finline. It is often necessary to be able to predict dispersion in such waveguides, and numerous analytical techniques have been developed for particular geometries. For example, the singular integral equation [1] and spectral-domain methods [2] have been used to find dispersion curves for planar waveguides with infinitely thin conductors. Of the techniques capable of analyzing arbitrary geometries, there has been some success with finite element and finite difference methods which use two axial field components as unknowns. However this approach cannot handle generally anisotropic materials and, more seriously, suffers from the presence of spurious solutions. For these reasons, a better approach is a vector method which uses the three-component magnetic field, $\boldsymbol{H}$, as the unknown [3].

Unfortunately, the transverse part of the magnetic or electric field is infinite at a sharp edge of a perfectly conducting boundary [4]. This is quite different from the behavior of the axial components, or of the potential used in quasi-static analysis [5]—these variables have infinite derivatives at such an edge, but are themselves finite. The three-component methods presented to date do not adequately address the problems that this singularity poses. The methods have used as basis functions the piecewise polynomials traditionally associated with finite elements. Such functions cannot represent accurately an infinite field. The solution proposed in this paper is to supplement the polynomials with singular trial functions.

Manuscript received March 25, 1988; revised August 25, 1988. This work was supported by the Natural Sciences and Engineering Council of Canada.

The author is with the Department of Electrical Engineering, McGill University, Montreal, H3A 2A7 Canada.

IEEE Log Number 8824338.

II. Variational Principle and Boundary Conditions

Assume that the electromagnetic field in the waveguide varies as $\exp(jk_0ct - j\beta z)$, where t is time, z is the distance along the guide axis, k_0 is the free-space wavenumber, c is the velocity of light in a vacuum, and β is the phase constant in the waveguide. This exponential factor will be omitted for brevity.

The vector finite element method finds the stationary points of the following functional [3], [6]:

$$F(\boldsymbol{H}) = \int_S \left[(\nabla \times \boldsymbol{H})^* \cdot \epsilon_r^{-1} \cdot (\nabla \times \boldsymbol{H}) + s|\nabla \cdot \mu_r \boldsymbol{H}|^2 - k_0^2 \boldsymbol{H}^* \cdot \mu_r \cdot \boldsymbol{H} \right] dS. \quad (1)$$

Here * denotes complex conjugate, S is the cross section of the waveguide, and ϵ_r and μ_r are the relative permittivity and permeability tensors. The second of the three terms in the functional is a penalty term, added to reduce the divergence of the magnetic flux density and hence to remove spurious modes [6], [7]. The parameter s is a real scalar, called the penalty parameter.

In finding the stationary points of F it is necessary to impose the boundary condition

$$\boldsymbol{H} \times \boldsymbol{n} = 0 \qquad \text{on } C_0 \quad (2)$$

where C_0 is a part of the perimeter of S corresponding to a perfect magnetic conductor, and $\boldsymbol{n}$ is a unit outward normal to the perimeter. The boundary conditions on perfectly conducting metal,

$$(\nabla \times \boldsymbol{H}) \times \boldsymbol{n} = 0 \quad (3)$$

and

$$\boldsymbol{H} \cdot \boldsymbol{n} = 0 \qquad \text{on } C_s$$

are satisfied naturally by stationary points of F, and it would not seem necessary to impose them. However, in order to eliminate spurious modes, the magnetic charge on C_s must be made small explicitly, for the same reason that the magnetic charge inside the waveguide must be reduced by using a penalty term [6], [7] or some other technique [8],

0018-9480/88/1200-1819$01.00

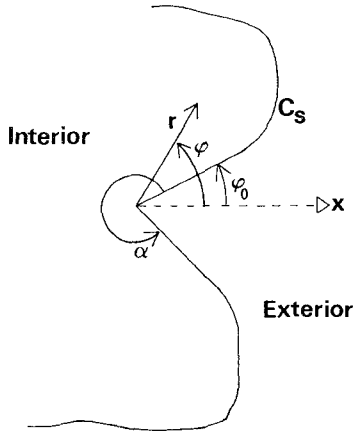

Fig. 1. The cylindrical coordinate system based on a sharp edge of a perfectly conducting boundary.

[9]. Therefore, the boundary condition

$$\boldsymbol{H}\cdot\boldsymbol{n}=0 \qquad \text{on } C_s \tag{4}$$

is imposed explicitly.

The stationary points $(\boldsymbol{H}, k_0)$ of F, subject to boundary conditions (2) and (4), are the modes of the waveguide which have the specified value of β. A similar functional and variational result exist for the electric field.

III. Singular Trial Functions

A typical sharp metal edge, and cylindrical coordinates based on it, are shown in Fig. 1. How should the boundary condition (4) be imposed at the edge, where there are two different normal vectors? One approach is to enforce

$$\boldsymbol{H}\cdot\boldsymbol{n}_{\text{av}}=0 \tag{5}$$

where $\boldsymbol{n}_{\text{av}}$ bisects the angle between the two normals. Note that if this is done, (4) will not be exactly satisfied along the two metal walls that meet at the edge. Another approach would be to leave the field free at the edge (presumably leaving it free at just a few boundary points in the problem would not introduce spurious modes). Finally, the transverse magnetic field could be set to zero there, which would at least satisfy (4) exactly along the two metal walls.

None of these approaches is entirely satisfactory because in fact the field is infinite at the edge. Let α be the interior angle, in radians, between π and 2π. The transverse magnetic field very close to the edge, when no magnetic material is present, is the gradient of a harmonic function which satisfies Neumann boundary conditions on the two conducting surfaces [4]. Starting from this, the transverse field $\boldsymbol{H}_t$ may be expressed as a series in powers of r, of which just the first m_0 terms are singular:

$$\boldsymbol{H}_t=\sum_{m=1}^{m_0} A_m \boldsymbol{f}_m(r,\varphi)+O(r) \tag{6}$$

where A_m are arbitrary coefficients and

$$\boldsymbol{f}_m=r^{mq-1}\left[\boldsymbol{a}_r\cos\left(mq(\varphi-\varphi_0)\right)-\boldsymbol{a}_\varphi\sin\left(mq(\varphi-\varphi_0)\right)\right] \tag{7}$$

$$q=\frac{\pi}{\alpha} \quad \text{and} \quad m_0=\text{int}\left[\frac{2}{q}\right]. \tag{8}$$

Here $\boldsymbol{a}_r$ and $\boldsymbol{a}_\varphi$ are unit vectors in the radial and azimuthal directions, respectively. There is a maximum of three singular functions $\boldsymbol{f}_m$ for each sharp edge. Of these, only the first is infinite at the edge; the remainder have infinite derivatives. A similar expansion is possible for the transverse electric field.

Suppose that for the problem as a whole, there are M such singular functions. Let these functions be $\boldsymbol{f}_i$, where i is now an index ranging from 1 to M. Then with respect to a given subdivision of the guide cross section into triangles, trial functions $\boldsymbol{g}_i$ are defined as follows:

$$\boldsymbol{g}_i(\boldsymbol{r})=\boldsymbol{f}_i(\boldsymbol{r})-\sum_{n=1}^{n_0}\boldsymbol{f}_{in}\alpha_n(\boldsymbol{r}), \qquad i=1,\cdots,M. \tag{9}$$

Here $\boldsymbol{r}$ is a vector denoting a point in the guide cross section; α_n are the usual n_0 Lagrange polynomials [10] associated with the triangle containing the point $\boldsymbol{r}$; and $\boldsymbol{f}_{in}$ is the value of $\boldsymbol{f}_i$ at the nth node of the triangle (zero if $\boldsymbol{f}_i$ is infinite at the nth node). The functions $\boldsymbol{g}_i$ are so constructed that they have the same behavior as the corresponding $\boldsymbol{f}_i$ near the latter's singular point, and they vanish at every other node of the finite element mesh. Note that each $\boldsymbol{g}_i$ extends over the whole cross section of the waveguide, but becomes increasingly small far from its singular point as the variation of $\boldsymbol{f}_i$ is better modeled by the polynomials in (9).

The singular functions $\boldsymbol{g}_i$ are used to supplement the polynomial trial functions over the mesh of triangles. Specifically, the magnetic field is taken to be

$$\boldsymbol{H}(\boldsymbol{r})=\sum_{n=1}^{n_0}\boldsymbol{H}_n\alpha_n(\boldsymbol{r})+\sum_{i=1}^{M}K_i\boldsymbol{g}_i(\boldsymbol{r}) \tag{10}$$

where $\boldsymbol{H}_n$ and K_i are unknown coefficients and, as before, α_n are the polynomials associated with the triangle containing point $\boldsymbol{r}$. In fact $\boldsymbol{H}_n$ is the magnetic field at node n of the triangle, provided none of the singular functions is infinite at the node.

IV. Evaluation of the Functional

The evaluation of the functional F for a magnetic field of the form (10) presents a few difficulties. The differentiation in (1) is relatively straightforward when it is noted that:

1) Differentiation with respect to z is just multiplication by $-j\beta$.

2)
$$\nabla\times\boldsymbol{f}_i=j\beta\boldsymbol{f}_i\times\boldsymbol{a}_z$$
$$\nabla\cdot\boldsymbol{f}_i=0 \tag{11}$$

where $\boldsymbol{a}_z$ is a unit vector along the guide axis.

3) The other derivatives in (1) can be dealt with by using the precalculated D matrices of Silvester [11]:

$$\frac{\partial \alpha_i}{\partial \zeta_p} = \sum_{j=1}^{n_0} D_{ij}^{(p)} \alpha_j, \qquad \text{for } i = 1, \cdots, n_0; \quad p = 1,2,3 \quad (12)$$

where ζ_p is the pth area coordinate in the triangle.

The integration in (1) reduces to the following integrals over each element S_e:

$$T_{ij} = \int_{S_e} \alpha_i \alpha_j \, dS, \qquad i = 1, \cdots, n_0; \; j = 1, \cdots, n_0 \quad (13)$$

$$I_{ij} = \int_{S_e} \sigma_i \alpha_j \, dS, \qquad i = 1, \cdots, M; \; j = 1, \cdots, n_0 \quad (14)$$

$$G_{ij} = \int_{S_e} \sigma_i \sigma_j \, dS, \qquad i = 1, \cdots, M; \; j = 1, \cdots, M \quad (15)$$

where σ_i, obtained from the x or y component of $\boldsymbol{f}_i$, is

$$\sigma_i = r^{mq-1} \begin{matrix} \cos \\ \sin \end{matrix} [mq(\varphi - \varphi_0) - \varphi]. \quad (16)$$

Notice that all of the integrands are of the form $U(\boldsymbol{r})V(\boldsymbol{r})$. T_{ij} can be readily computed from the area of the triangle and precalculated universal T matrices [11]. The other two integrals must be evaluated numerically. If the integrand is not singular in the element S_e, then appropriate Gauss quadrature formulas are used [12]. If the integrand is singular in the triangle, it is first expressed as the sum of a singular part, $W(\boldsymbol{r})$, and a nonsingular part, $UV - W$. Let $\boldsymbol{r}_u$ be the point at which U is singular, and let $\boldsymbol{r}_v$ be the point at which V is singular. There are four cases to consider, depending on whether these points are in the triangle or not:

If U is singular in the triangle and V is not:

$$W(\boldsymbol{r}) = U(\boldsymbol{r})V(\boldsymbol{r}_u). \quad (17a)$$

If V is singular in the triangle and U is not:

$$W(\boldsymbol{r}) = V(\boldsymbol{r})U(\boldsymbol{r}_v). \quad (17b)$$

If both U and V are singular in the triangle, at different points:

$$W(\boldsymbol{r}) = U(\boldsymbol{r})V(\boldsymbol{r}_u) + V(\boldsymbol{r})U(\boldsymbol{r}_v). \quad (17c)$$

If both U and V are singular in the triangle, at the same point:

$$W(\boldsymbol{r}) = U(\boldsymbol{r})V(\boldsymbol{r}). \quad (17d)$$

In each case $UV - W$ is nonsingular and can be integrated with Gauss formulas [12].

Also, in each case, W is of the form

$$r^b h(\varphi), \qquad -1 \leqslant b \leqslant 0 \quad (18)$$

where (r, φ) are cylindrical coordinates based on one of the sharp edges, coincident with a vertex of the triangle, and h is a bounded function of φ only. Then, with R, H, φ_1, φ_2, and θ as indicated in Fig. 2,

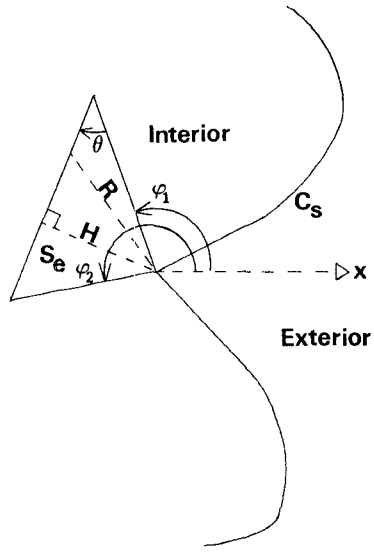

Fig. 2. A triangle with a vertex at a sharp edge. (The other triangles in the interior of the waveguide are omitted.)

$$\int_{S_e} r^b h(\varphi) \, dS = \int_{\varphi=\varphi_1}^{\varphi_2} \int_{r=0}^{R(\varphi)} r^b h(\varphi) \, r \, d\varphi \, dr = \frac{1}{b+2} \int_{\varphi=\varphi_1}^{\varphi_2} [R(\varphi)]^{(b+2)} h(\varphi) \, d\varphi \quad (19)$$

where $R(\varphi)$ is

$$R(\varphi) = \frac{H}{\sin(\varphi - \varphi_1 + \theta)}. \quad (20)$$

The integrand in (19) is nonsingular and can be integrated with 1-D Gauss formulas.

Finally, the contribution to the functional from the eth triangle can be written

$$F^{(e)} = \boldsymbol{x}^{(e)H} \left[\boldsymbol{A}^{(e)} + s\boldsymbol{C}^{(e)} - k_0^2 \boldsymbol{B}^{(e)} \right] \boldsymbol{x}^{(e)} \quad (21)$$

where the superscript e denotes the eth element, and the superscript H stands for complex-conjugate transpose; $\boldsymbol{x}^{(e)}$ is a column vector whose entries are the $3n_0$ Cartesian components of the magnetic field at the nodes, and the M unknown coefficients K_i. $\boldsymbol{A}^{(e)}$, $\boldsymbol{B}^{(e)}$, and $\boldsymbol{C}^{(e)}$ are $(3n_0 + M)$ by $(3n_0 + M)$ Hermitian matrices.

The functional F is the sum of contributions from all the triangles of the cross section S, and can be written

$$F = \boldsymbol{x}^H \left[\boldsymbol{A} + s\boldsymbol{C} - k_0^2 \boldsymbol{B} \right] \boldsymbol{x} \quad (22)$$

where $\boldsymbol{A}$, $\boldsymbol{B}$, and $\boldsymbol{C}$ are large, sparse, square, Hermitian matrices, and $\boldsymbol{x}$ is a column vector whose entries are all the unknown components of the magnetic field at the nodes, and the coefficients K_i.

The boundary conditions (2) and (4) are enforced either by expressing one Cartesian field component in terms of another or by setting components to zero at each boundary node. Both transverse components of the magnetic field are set to zero at a node at a sharp edge, in order to satisfy the boundary condition (4) along the metal walls that meet there. The result is that the column vector $\boldsymbol{x}$ can be written

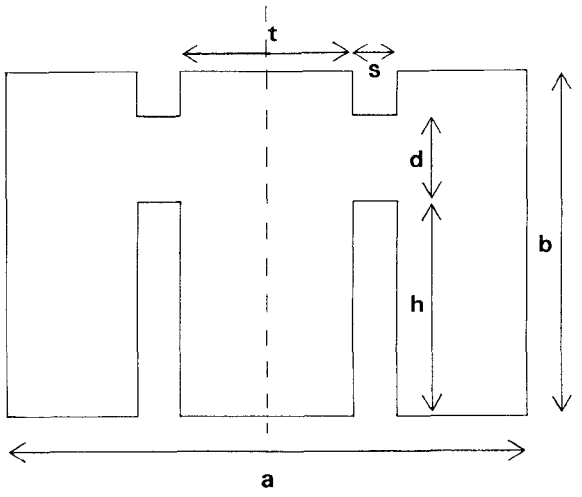

Fig. 3. Rectangular waveguide with two double ridges. $b/a = 0.5$, $d/b = 0.1$, $s/a = 0.125$, $h/b = 0.7$, $t/a = 0.5$. The broken line is a plane of symmetry.

in terms of a smaller vector y containing just those components and coefficients that are nonzero and independently variable:

$$x = Ry \tag{23}$$

where R is a real, rectangular matrix. Then

$$F = y^H \left[A' + sC' - k_0^2 B' \right] y \tag{24}$$

where A' is the reduced matrix $R^T A R$; the same is true for B' and C'.

V. The Algebraic Eigenvalue Problem

The stationary points of the functional F are given by the eigensolutions of the matrix equation:

$$(A' + sC')\, y = k_0^2 B' y \tag{25}$$

Efficient methods exist for finding the first few eigenvalues and corresponding eigenvectors of this sparse matrix equation; in the present instance, trace minimization is used [13]. This method requires the storage and manipulation of only the nonzero entries of the matrices and has a complexity which is roughly $O(N^{1.5})$, where N is the matrix dimension. To find the lowest two modes when the matrix dimension is 450 and there are about 33 nonzeros per row in each matrix takes about 20 minutes of CPU time on an HP 9000 Series 500 computer.

A modification of the algorithm [14] allows for the automatic adjustment of the penalty parameter s during solution, to eliminate spurious modes. However, when just the slow-wave region is of interest, it is sufficient to hold the penalty parameter fixed at 1.0 [15]. This approach was taken for the microstrip problems below.

VI. Results

Fig. 3 shows a rectangular waveguide with two double ridges. This structure is air-filled and has modes which are TE or TM, so it could be more efficiently analyzed with a single axial component of E or H. However, it was chosen as a test problem because it has eight sharp edges (four in the half problem).

TABLE I
Cutoff Wavenumber, k_0 (rad/m) for the First Two Modes of the Waveguide Shown in Fig. 3

Mode	F. E. Solution		Ref. [16]
	Magnetic	Electric	
Dominant	0.923	0.904	0.911
Subdominant	1.177	1.150	1.161

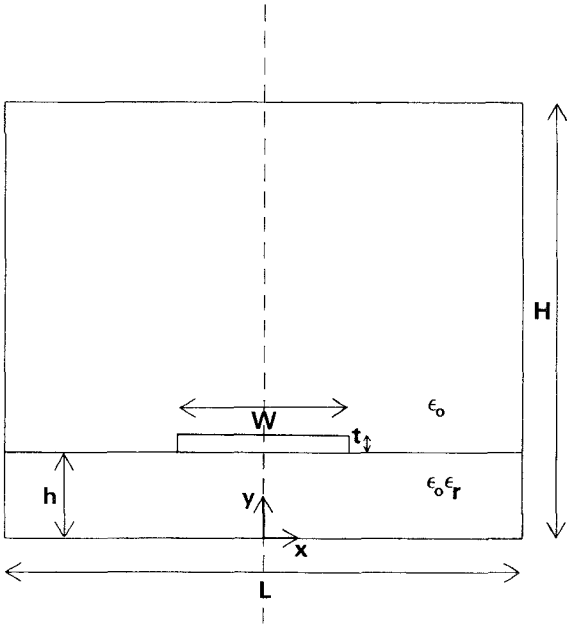

Fig. 4. A shielded microstrip transmission line. The broken line shows the plane of symmetry. $L = 12.7$ mm, $W = 1.27$ mm, $h = 1.27$ mm, $H = 12.7$ mm.

One half of the problem was analyzed at cutoff ($\beta = 0$), using 42 second-order elements and eight singular trial functions. To get the two lowest modes, it was necessary to solve two problems: one with an electric wall and one with a magnetic wall on the plane of symmetry. Each problem was analyzed twice, once with the magnetic field as the unknown and once with the electric field. The lowest two modes are TE and therefore at cutoff they have only an axial component of the magnetic field. The electric field is more interesting, because it is transverse and infinite at the sharp edges. The cutoff frequencies have been previously obtained with an accuracy of about 1 percent [16]. See Table I.

The electric field cases were also solved without singular trial functions, but with the field constrained by (5) at each sharp edge. The first two wavenumbers were extremely inaccurate: 3.05 rad/m and 3.23 rad/m, respectively.

A second test problem was the shielded microstrip shown in Fig. 4. One half of the problem was analyzed, with a magnetic wall on the plane of symmetry. A total of 73

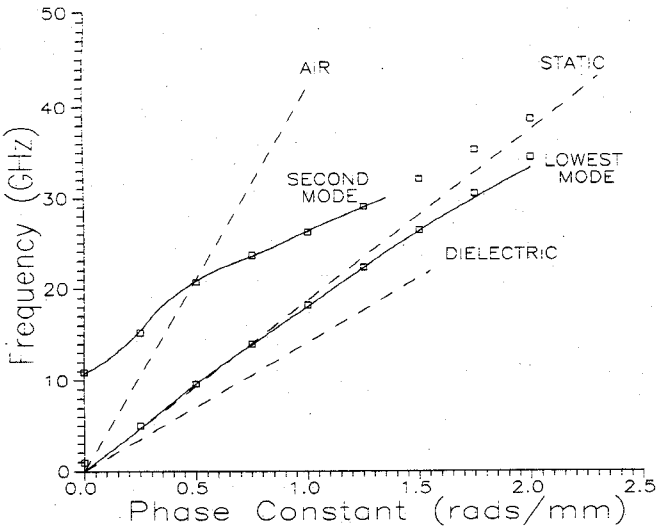

Fig. 5. Dispersion curves for the first two modes of the transmission line of Fig. 4, with a magnetic wall at the plane of symmetry. Isotropic substrate, $\epsilon_r = 8.875$. $t = 0$. The solid line for the lowest mode is from [1]; the solid line for the next mode is from [17]; squares are finite element results. The broken line marked AIR is the dispersion curve for a uniform plane wave in free space; the broken line marked DIELECTRIC is the dispersion curve for a uniform plane wave in the substrate. The broken line marked STATIC is the low-frequency approximation for the dominant mode (from Wheeler [18]).

TABLE II
COMPUTED FREQUENCIES AT TWO VALUES OF PHASE CONSTANT FOR THREE CASES CORRESPONDING TO DIFFERENT BOUNDARY CONDITIONS IMPOSED ON THE SHARP EDGE OF THE MICROSTRIP SHOWN IN FIG. 4

Case	Frequency (GHz)	
	β = 0	β = 2 rads/mm
A	12.82	37.21
B	11.81	36.91
C	0.95	34.42

second-order elements were used (most of them placed close to the central conducting strip). The results are plotted in Fig. 5. Table II demonstrates that if singular trial functions are not used, a considerable overestimation of the frequencies results. For case A, (5) was enforced; for case B, the field at the node on the sharp edge was allowed to vary freely; for case C, singular functions were used.

The same microstrip line was then solved with an anisotropic substrate. The results are shown in Fig. 6.

VII. CONCLUSIONS

The vector finite element method presented is an effective way to predict dispersion in arbitrary waveguides with sharp metal edges. The success of the method is largely due to the use of special trial functions which model the singular behavior of the field close to sharp edges.

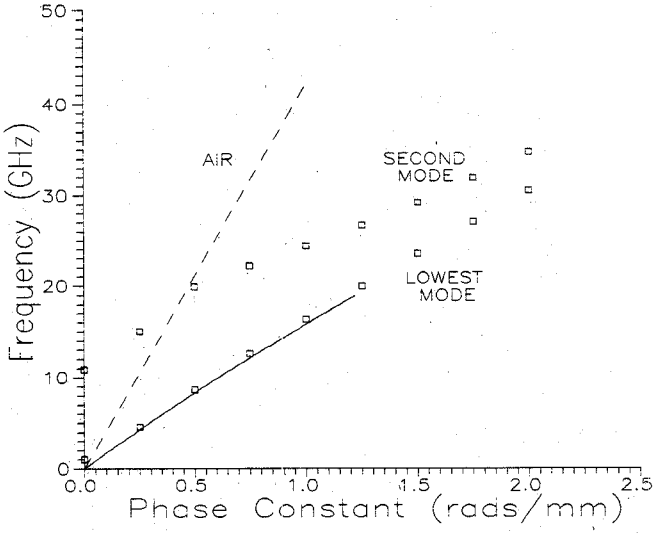

Fig. 6. Dispersion curves for the first two modes of the transmission line of Fig. 4, with a magnetic wall at the plane of symmetry. Sapphire substrate: $\epsilon_{rxx} = 9.4$, $\epsilon_{ryy} = 11.6$, and $\epsilon_{rzz} = 9.4$, $t = 0$. The solid line for the lowest mode is from [19], with no shield present. The squares are the finite element results.

ACKNOWLEDGMENT

The author is grateful to Infolytica Corporation for the use of their finite element pre- and post-processing software.

REFERENCES

[1] R. Mittra and T. Itoh, "A new technique for the analysis of the dispersion characteristics of microstrip line," *IEEE Trans. Microwave Theory Tech.*, vol. MTT-19, pp. 47–56, Jan. 1971.

[2] T. Itoh and R. Mittra, "Spectral-domain approach for calculating the dispersion characteristics of microstrip lines," *IEEE Trans. Microwave Theory Tech.*, vol. MTT-21, pp. 496–499, July 1973.

[3] B. M. A. Rahman and J. B Davies, "Finite element analysis of optical and microwave problems," *IEEE Trans. Microwave Theory Tech.*, vol. MTT-32, pp. 20–28, Jan. 1984.

[4] J. Van Bladel, "Field singularities at metal–dielectric wedges," *IEEE Trans. Antennas Propagat.*, vol. AP-33, pp. 450–455, April 1985.

[5] Z. Pantic and R. Mittra, "Quasi-TEM analysis of microwave transmission lines by the finite-element method," *IEEE Trans. Microwave Theory Tech.*, vol. MTT-34, pp. 1096–1103, Nov. 1986.

[6] B. M. A. Rahman and J. B. Davies, "Penalty function improvement of waveguide solution by finite elements," *IEEE Trans. Microwave Theory Tech.*, vol. MTT-32, pp. 922–928, Aug. 1984.

[7] J. P. Webb, "The finite element method for finding modes of dielectric-loaded cavities," *IEEE Trans. Microwave Theory Tech.*, vol. MTT-33, pp. 635–639, July 1985.

[8] A. Konrad, "A direct three-dimensional finite element method for the solution of electromagnetic fields in cavities," *IEEE Trans. Magn.*, vol. MAG-21, pp. 2276–2279, Nov. 1985.

[9] A. J. Kobelansky and J. P. Webb, "Eliminating spurious modes in finite-element waveguide problems by using divergence-free fields," *Electron. Lett.*, vol. 22, no. 11, pp. 569–570, May 22, 1986.

[10] P. Silvester and R. L. Ferrari, *Finite Elements for Electrical Engineers*. New York: Cambridge University Press, 1983.

[11] P. Silvester, "Construction of triangular finite element universal matrices," *Int. J. Numer. Meth. Eng.*, vol. 12, pp. 237–244, 1978.

[12] D. A. Dunavant, "High degree efficient symmetrical Gaussian quadrature rules for the triangle," *Int. J. Numer. Meth. Eng.*, vol. 21, pp. 1129–1148, 1985.

[13] A. H. Sameh and J. A. Wisniewski, "A trace minimization algorithm for the generalized eignvalue problem," *SIAM J. Numer. Anal.*, vol. 19, no. 6, pp. 1243–1259, Dec. 1982.

[14] J. P. Webb, "Efficient generation of divergence-free fields for the finite element analysis of 3D cavity resonances," *IEEE Trans. Magn.*, vol. 24, pp. 162–165, Jan. 1988.
[15] M. Koshiba, K. Hayata, and M. Suzuki, "Improved finite-element formulation in terms of the magnetic vector for dielectric waveguides," *IEEE Trans. Microwave Theory Tech.*, vol. MTT-33, pp. 227–233, Mar. 1985.
[16] D. Dasgupta and P. K. Saha, "Rectangular waveguide with two double ridges," *IEEE Trans. Microwave Theory Tech.*, vol. MTT-31, pp. 938–941, Nov. 1983.
[17] D. Mirshekar-Syahkal and J. B. Davies, "Accurate solution of microstrip and coplanar structures for dispersion and for dielectric and conductor losses," *IEEE Trans. Microwave Theory Tech.*, vol. MTT-27, pp. 694–699, July 1979.
[18] H. A. Wheeler, "Transmission-line properties of a strip on a dielectric sheet on a plane," *IEEE Trans. Microwave Theory Tech.*, vol. MTT-25, pp. 631–643, Aug. 1977.
[19] B. E. Kretch and R. E. Collin, "Microstrip dispersion including anisotropic substrates," *IEEE Trans. Microwave Theory Tech.*, vol. MTT-35, pp. 710–718, Aug. 1987.

✠

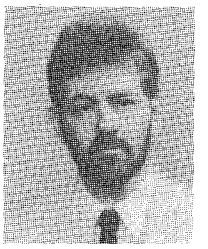

J. P. Webb (M'83) received the Ph.D. degree from Cambridge University, England, in 1981. The subject of his thesis was a three-dimensional finite-element method for finding electromagnetic fields in microwave cavities.

Since 1982 he has been an Assistant Professor, then an Associate Professor, in the Electrical Engineering Department of McGill University, Montreal, Canada. His area of research is computer methods in electromagnetics, especially the application of the finite element method.